Received: 2 May 2022 | Revised: 28 July 2022 | Accepted: 6 August 2022

DOI: 10.1111/cas.15530

ORIGINAL ARTICLE

Cancer Science WILEY

α1,4-Linked *N*-acetylglucosamine suppresses gastric cancer development by inhibiting Mucin-1-mediated signaling

Chifumi Fujii[1,2] | Satoru Harumiya[1] | Yoshiko Sato[1] | Masatomo Kawakubo[1] | Hisanori Matoba[1] | Jun Nakayama[1]

[1]Department of Molecular Pathology, Shinshu University School of Medicine, Matsumoto, Japan

[2]Department of Biotechnology, Institute for Biomedical Sciences, Interdisciplinary Cluster for Cutting Edge Research, Shinshu University, Matsumoto, Japan

Correspondence
Chifumi Fujii, Department of Molecular Pathology, Shinshu University School of Medicine, and Department of Biotechnology, Institute for Biomedical Sciences, Interdisciplinary Cluster for Cutting Edge Research, Shinshu University, 3-1-1 Asahi, Matsumoto 390-8621, Japan.
Email: chifumif@shinshu-u.ac.jp

Funding information
Japan Society for the Promotion of Science, Grant/Award Number: 18K08613 and 19H03441

Abstract

Gastric cancer is the second leading cause of cancer deaths worldwide, and more understanding of its molecular basis is urgently needed. Gastric gland mucin secreted from pyloric gland cells, mucous neck cells, and cardiac gland cells of the gastric mucosa harbors unique *O*-glycans carrying terminal α1,4-linked *N*-acetylglucosamine (αGlcNAc) residues. We previously reported that αGlcNAc loss correlated positively with poor outcomes for patients with differentiated-type gastric cancer. However, the molecular mechanisms underlying these outcomes remained poorly understood. Here, we examined the effects of upregulated αGlcNAc expression on malignant phenotypes of the differentiated-type gastric cancer cell lines, AGS and MKN7. Upregulation of αGlcNAc following ectopic expression of its biosynthetic enzyme attenuated cell proliferation, motility, and invasiveness of AGS and MKN7 cells in vitro. Moreover, AGS cell tumorigenicity was significantly suppressed by αGlcNAc overexpression in a xenograft model. To define the molecular mechanisms underlying these phenotypes, we investigated αGlcNAc binding proteins in AGS cells and identified Mucin-1 (MUC1) and podocalyxin. Both proteins were colocalized with αGlcNAc on human gastric cancer cells. We also found that αGlcNAc was bound to MUC1 in murine normal gastric mucosa. When we assessed the effects of αGlcNAc binding to MUC1, we found that αGlcNAc blocked galectin-3 binding to MUC1, phosphorylation of the MUC1 C-terminus, and recruitment of Src and β-catenin to that C-terminus. These results suggest that αGlcNAc regulates cancer cell phenotypes by dampening MUC1 signal transduction.

KEYWORDS
differentiated-type gastric cancer, invasion, malignant phenotype, tumor suppressor, αGlcNAc-binding protein

1 | INTRODUCTION

Malignant neoplasms are leading causes of death in every country in the world and are important factors in decreasing life expectancy.[1] According to WHO estimates for 2019, malignant neoplasms are the leading or second highest cause of death before the age of 70 in 112 of 183 countries, and rank as third or fourth in another 23 countries.[2] Among them, gastric cancer is the second leading cause of

Abbreviations: αGlcNAc, α1,4-linked *N*-acetylglucosamine; α4GnT, α1,4-*N*-acetylglucosaminyltransferase; Dox, doxycycline; GSL II, *Griffonia (Bandieraea) simplicifilia* lectin II; IP, immunoprecipitation; MUC1, Mucin-1; MUC1-C, MUC1-C terminus; MUC1-N, MUC1-N terminus; PODXL, podocalyxin; WB, Western blotting.

cancer death worldwide.[3] Therefore, it is important to understand the biology of gastric cancer in order to develop useful prognostic factors or more effective therapeutic approaches.

Recent molecular analyses have identified multiple factors that regulate progression, invasion, and metastasis of gastric tumors. Gastric gland mucin secreted from pyloric gland cells, mucous neck cells, and cardiac gland cells of the gastric mucosa harbors unique *O*-glycans carrying terminal αGlcNAc residues.[4–6] We previously used expression cloning to isolate cDNA encoding α4GnT and revealed it to be a key enzyme catalyzing αGlcNAc biosynthesis.[7] When we generated *A4gnt* KO mice, we found that they completely lacked αGlcNAc and spontaneously developed differentiated-type adenocarcinoma in the pyloric mucosa through a hyperplasia–dysplasia–carcinoma sequence.[8] We also observed that αGlcNAc was frequently lost in differentiated-type gastric adenocarcinoma in humans and that loss was significantly associated with tumor invasion depth, venous invasion, and poor prognosis.[9] Furthermore, in human gastric atrophy and human pyloric gland-type adenoma, decreased αGlcNAc levels correlated with malignant potential.[10–12] However, the mechanistic basis for those findings were unknown.

Here, to address that question, we examined effects of forced αGlcNAc upregulation on malignant phenotypes of the moderately differentiated gastric cancer cell line, AGS, as well as the well differentiated gastric cancer cell line, MKN7. To do so, in both lines, we ectopically expressed α4GnT using the Tet-On system and assessed their phenotypes in vitro and in a xenograft model. Collectively, in both lines, we observed that αGlcNAc overexpression had tumor-suppressive effects. We also report the molecular mechanisms that likely underlie αGlcNAc-mediated tumor suppressive phenotypes.

2 | MATERIALS AND METHODS

Detailed methods, including establishment of α4GnT-expressing cells using the Tet-On system, analysis of cellular phenotype in vitro, in vivo tumorigenesis assay, identification of αGlcNAc-binding protein, IP, fluorescent immunohistochemistry, and statistical analysis, can be found in Appendix S1.

3 | RESULTS

3.1 | Establishment of α4GnT-overexpressing AGS cells using the Tet-On system

To assess effects of αGlcNAc on malignancy, we ectopically expressed the gene encoding α4GnT in gastric cancer cell lines as a means to increase αGlcNAc biosynthesis. To do so, we used the Tet-On system to drive ectopic α4GnT expression in both AGS, a human moderately differentiated gastric cancer line, and MKN7, a human well differentiated gastric cancer line. Expression of α4GnT was confirmed as induced by Dox treatment by WB analysis (Figures 1A and S1A). Flow cytometric analysis showed that

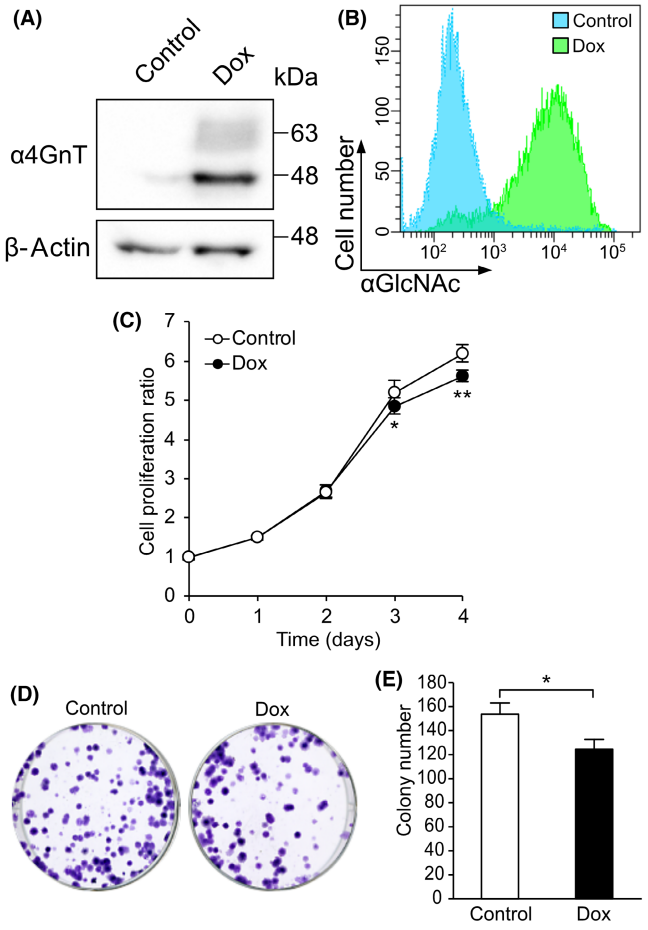

FIGURE 1 Establishment of AGS-A cells and analysis of their proliferation in vitro. (A) Western blot analysis of α1,4-*N*-acetylglucosaminyltransferase (α4GnT) following doxycycline (Dox) induction using the Tet-On system. β-Actin served as loading control. (B) Evaluation of cell surface αGlcNAc expression by flow cytometry. (C) Proliferation analysis based on an MTS assay. The proportion of cells relative to that seen on day 0 was calculated daily, with the value seen on day 0 set to 1. Results are indicated as means, and error bars indicate SD ($n = 6$). Representative results from three independent experiments are shown. (D,E) Anchorage-dependent colony formation assay. (D) Representative photographs of crystal violet-stained cells are shown. (E) Quantification of colony numbers. Results are indicated as means, and error bars indicate SD ($n = 3$). Representative results from three independent experiments are shown. $^{*}p < 0.05$, $^{**}p < 0.01$.

αGlcNAc was expressed on the cell surface in more than 90% of Dox-treated AGS cells (Figure 1B) and more than 70% of Dox-treated MKN7 cells (Figure S1B). We designated established cells as "AGS-A" or "MKN7-A" and used them for further study.

3.2 | Upregulation of αGlcNAc mildly attenuates cell proliferation in vitro

We initially evaluated cellular proliferation by quantifying cell proliferation in vitro using an MTS assay. In AGS-A cells, the proportion of

proliferating cells relative to controls began to significantly decline starting at 3–4 days after initiating Dox treatment under standard culture conditions (Figure 1C). MKN7-A cells showed similar effects (Figure S1C). Analysis using an anchorage-dependent clonogenic assay confirmed that the colony formation capacity of AGS-A cells was significantly attenuated relative to controls in the presence of Dox until day 13 (Figure 1D,E). Likewise, in MKN7-A cells, we observed a mild decrease in anchorage-dependent colony formation relative to control cells, but that decrease was not significant (Figure S1D,E). These findings indicate that upregulated αGlcNAc biosynthesis mildly but significantly attenuates proliferation of these gastric cancer cell lines in vitro and attenuates anchorage-dependent clonogenicity of AGS cells.

3.3 | Upregulated αGlcNAc biosynthesis significantly suppresses cellular motility and invasiveness in vitro

We next assessed the effects of αGlcNAc on gastric cancer malignancy by examining metastatic phenotypes in vitro in our αGlcNAc-overexpressing cell lines. As shown in Figure 2A, adherence of

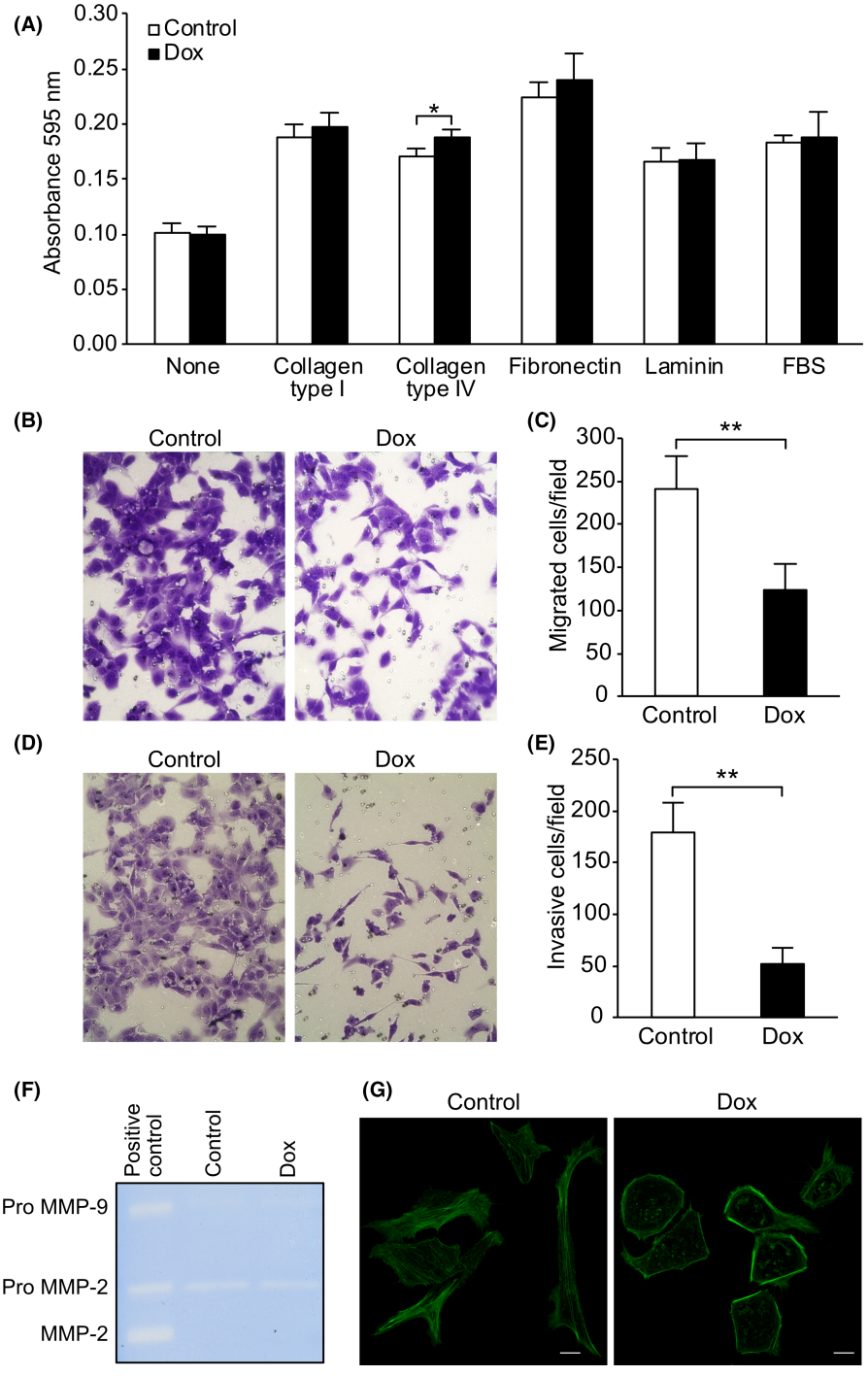

FIGURE 2 In vitro metastatic phenotypes of AGS-A cells. (A) Analysis of adhesion to ECM. After precoating 96-well plates with indicated ECM components, adhesion assays were carried out. Results are indicated as means ($n = 4$), and error bars indicate SD. Representative results from three independent experiments are shown. (B,C) Transwell migration assay. (B) Representative photographs of crystal violet-stained migrated cells in the presence or absence of doxycycline (Dox). (C) Quantification of cell migration. Migrated cells were observed by light microscopy (×200 magnification) and counted in five randomly selected fields from triplicate wells. Results are expressed as means ($n = 15$), and error bars indicate SD. Representative results from three independent experiments are shown. (D,E) Matrigel invasion assay. (D) Representative photographs of crystal violet-stained invasive cells in the presence or absence of Dox. (E) Quantification of cell invasiveness. Invasive cells were observed by light microscopy (×200 magnification) and counted in five randomly selected fields from triplicate wells. Results are expressed as means ($n = 15$) and error bars indicate SD. Representative results from three independent experiments are shown. (F) Gelatin zymography. (G) Morphological changes in the cytoskeleton seen in Dox-treated AGS-A cells. F-actin was visualized by staining with Acti-stain 488 fluorescent phalloidin and observed by confocal microscopy. Representative photographs are shown. Scale bar, 10 μm. $^{*}p < 0.05$, $^{**}p < 0.01$.

AGS-A cells onto collagen type I, collagen type IV, fibronectin, or laminin was not affected by Dox treatment. We then assessed AGS-A cell motility using a Transwell migration assay and found it significantly attenuated in Dox-treated cells relative to control cells (Figure 2B,C). Analysis of AGS-A cell invasiveness based on a Matrigel invasion assay indicated that the number of invaded cells

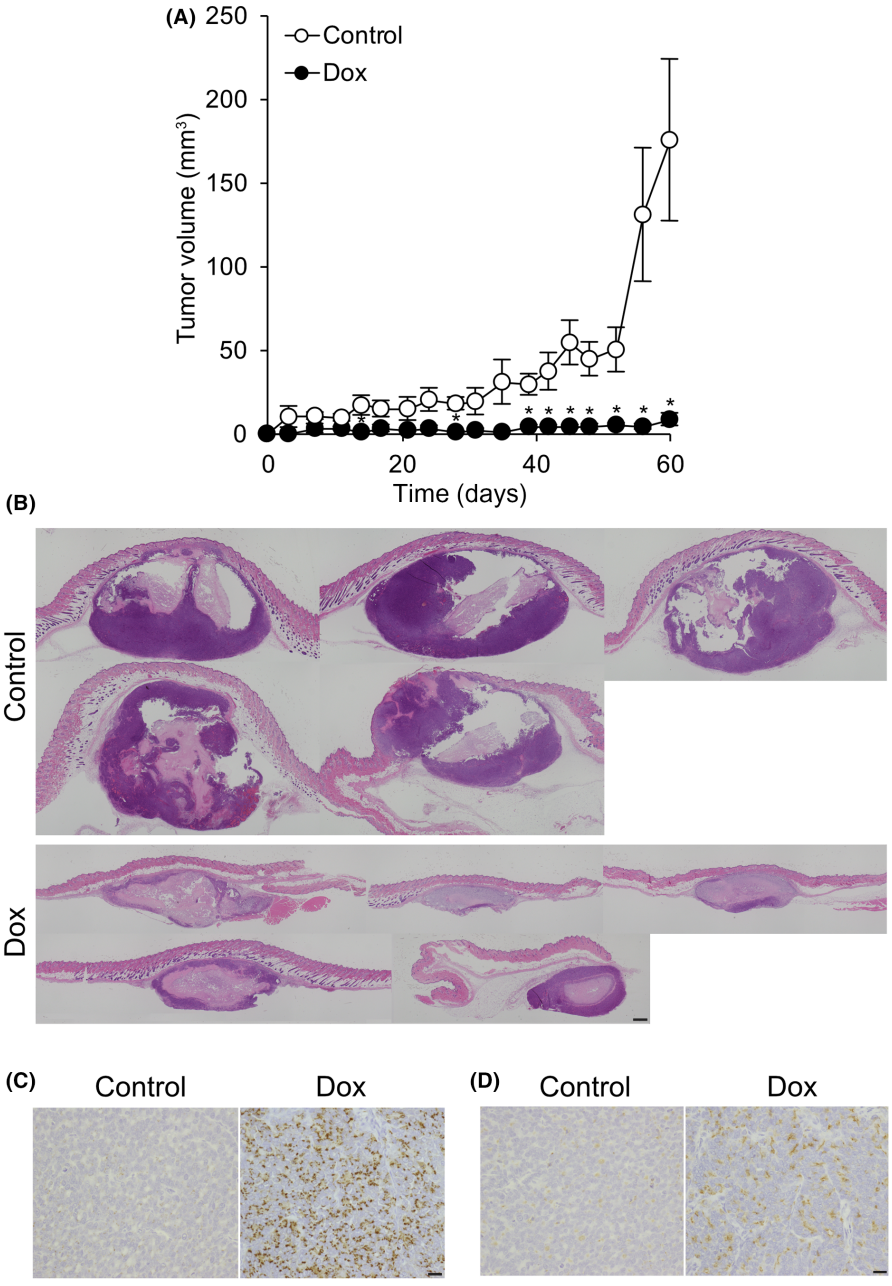

FIGURE 3 Analysis of in vivo tumorigenesis in a xenograft model. (A) NOD.CB17-Prkdc^{scid}/J mice were implanted subcutaneously in the flank with AGS-A cells and doxycycline (Dox) was given in drinking water. Tumor size was measured at indicated time points. Results are expressed as means ($n = 5$), and error bars indicate SE. Representative results from three independent experiments are shown. $^{*}p < 0.05$. (B) H&E staining of tumor cross-sections. Scale bar, 500 μm. (C,D) Immunohistochemistry for (C) α1,4-*N*-acetylglucosaminyltransferase or (D) α1,4-linked *N*-acetylglucosamine. Scale bar, 20 μm.

FIGURE 4 Identification of α1,4-linked *N*-acetylglucosamine (αGlcNAc)-binding proteins in AGS-A cells. (A,B) Silver-stained gel of SDS-PAGE (A) and western blotting (B) analysis of eluates of *Griffonia (Bandieraea) simplicifilia* lectin II pull-down products by *N*-acetylglucosamine. Arrowheads indicate bands present only in doxycycline (Dox)-treated cells and whose mobility is identical to that seen in western blotting. (C,D) Immunoprecipitation (IP) and western blot analysis of αGlcNAc binding to (C) Mucin-1 (MUC1) or (D) podocalyxin (PODXL). Whole cell lysates (WCL) of AGS-A cells were immunoprecipitated and immunoblotted with indicated Abs. Arrowheads indicate αGlcNAc-bound (C) MUC1 or (D) PODXL. (E) Immunocytochemical analysis of MUC1 and αGlcNAc in AGS-A cells. Upper panels, control cells; lower panels, Dox-treated cells. Scale bar, 10 μm. (F) Fluorescent immunohistochemical analysis of MUC1 (red) and αGlcNAc (green) in human gastric cancer tissue. Upper panels show original magnification at ×100, and lower represent enlargements of regions contained within squares in upper panels. Left panels show H&E staining. Scale bar, 100 μm. (G) Immunocytochemical analysis of PODXL and αGlcNAc in AGS-A cells. Upper panels, control cells; lower panels, Dox-treated cells. Scale bar, 10 μm. (H) Fluorescent immunohistochemical analysis of PODXL (red) and αGlcNAc (green) in human gastric cancer tissue. Upper panels show original magnification at ×100, and lower represent enlargements of regions contained within squares in upper panels. Left panels show H&E staining. Scale bar, 100 μm.

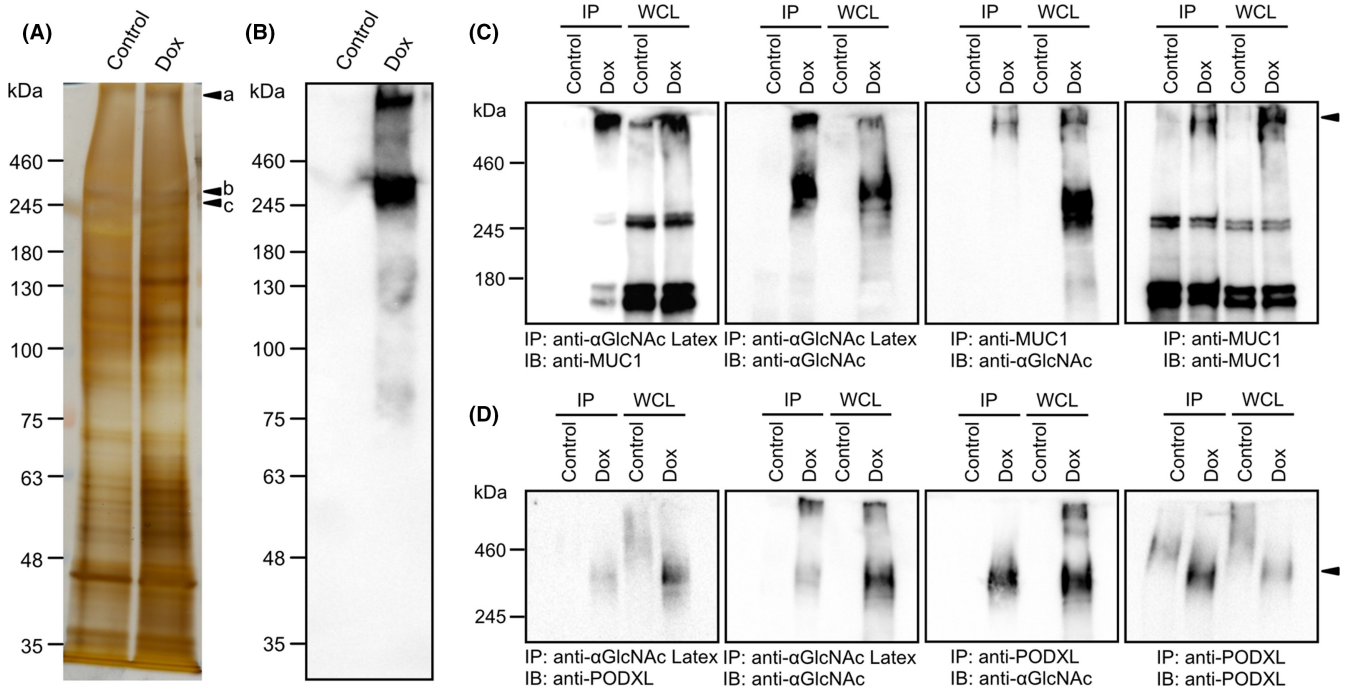
(A)
Control
Dox
kDa
460
245
180
130
100
75
63
48
35
a
b
c
(B)
Control
Dox
kDa
460
245
180
130
100
75
63
48
35
(C)
IP
WCL
Control
Dox
kDa
460
245
180
IP: anti-αGlcNAc Latex
IB: anti-MUC1
IP: anti-αGlcNAc Latex
IB: anti-αGlcNAc
IP: anti-MUC1
IB: anti-αGlcNAc
IP: anti-MUC1
IB: anti-MUC1
(D)
IP
WCL
Control
Dox
kDa
460
245
IP: anti-αGlcNAc Latex
IB: anti-PODXL
IP: anti-αGlcNAc Latex
IB: anti-αGlcNAc
IP: anti-PODXL
IB: anti-αGlcNAc
IP: anti-PODXL
IB: anti-PODXL

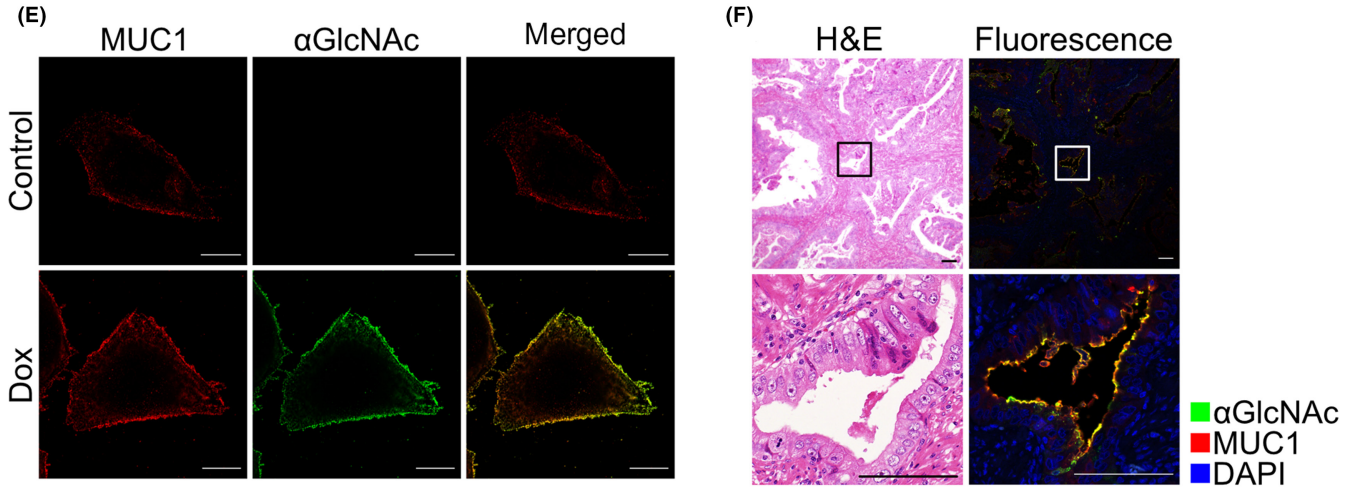
(E)
MUC1
αGlcNAc
Merged
Control
Dox
(F)
H&E
Fluorescence
αGlcNAc
MUC1
DAPI

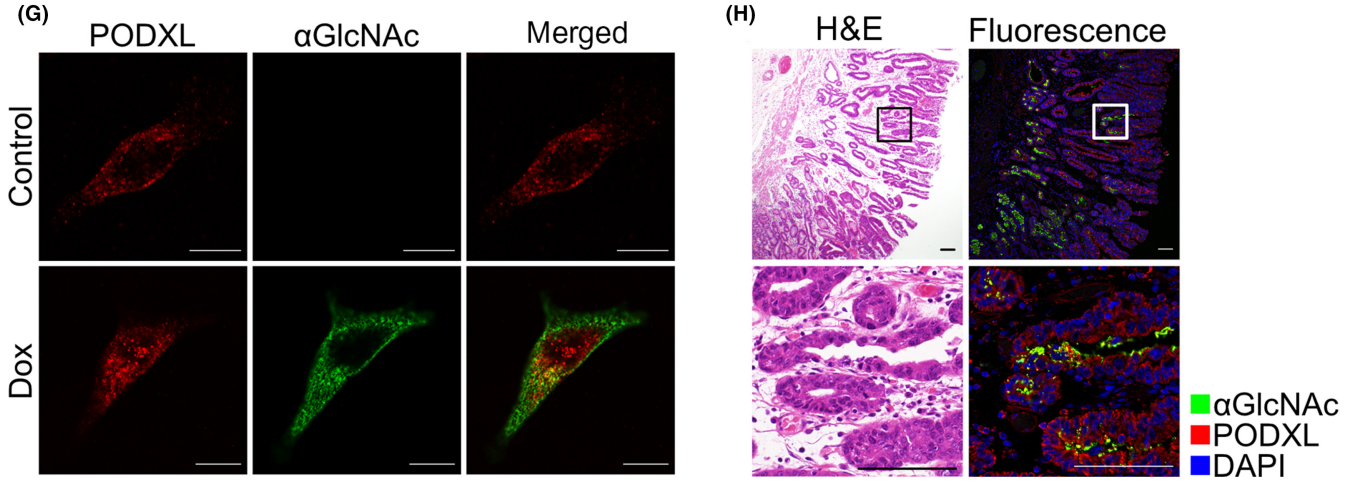
(G)
PODXL
αGlcNAc
Merged
Control
Dox
(H)
H&E
Fluorescence
αGlcNAc
PODXL
DAPI

significantly decreased in the presence of Dox relative to controls (Figure 2D,E). We observed comparable outcomes in terms of both motility and invasiveness in MKN7-A cells (Figure S2). To determine the relevant mechanism, we undertook gelatin zymography to assess MMP levels and activities. We observed comparable pro-MMP-9 and pro-MMP-2 secretion levels in AGS-A cell conditioned medium with or without Dox and did not detect active MMP-2 (Figure 2F). Given that reduced invasiveness was apparently not due to MMP-dependent ECM degradation, we analyzed formation of the cellular cytoskeleton by cultivating AGS-A cells on Matrigel-coated coverslips treated with or without Dox, and then analyzing F-actin by phalloidin staining. Relative to untreated controls, Dox-treated AGS-A cells did not undergo cytoskeletal remodeling (Figure 2G). These results suggest that αGlcNAc biosynthesis attenuates malignant phenotypes of gastric cancer cells.

3.4 | Enhanced αGlcNAc biosynthesis significantly attenuates tumorigenesis in a xenograft model

We next assessed the effects of upregulated αGlcNAc biosynthesis on tumorigenesis using a xenograft model. To do so, we inoculated immunodeficient mice with AGS-A cells that had been treated with or without Dox and then continued to administer Dox in drinking water to mice transplanted with the Dox-treated cells. Over a 60-day observation period, tumor volume in the Dox-treated group was significantly reduced relative to controls (Figure 3A). Histologically, most tumor cells in the Dox group were necrotic, while most tumor cells in the control group appeared to remain viable (Figure 3B). Expression of α4GnT in tumor cells of Dox-treated mice was confirmed by immunohistochemistry using an anti-α4GnT Ab (Figure 3C), and immunohistochemistry using an anti-αGlcNAc Ab confirmed upregulated αGlcNAc expression in the Dox group (Figure 3D). These results together suggest that αGlcNAc biosynthesis attenuates tumorigenesis of AGS-A cells.

3.5 | Identification of αGlcNAc-binding proteins in AGS cells

We next investigated the molecular basis of antimalignant phenotypes promoted by αGlcNAc overproduction in AGS-A and MKN7-A cells. α1,4-Linked *N*-acetylglucosamine primarily binds at the terminal glycosylated residue to scaffold protein MUC6[4–6]; however, MUC6 is not expressed in AGS or MKN7 cells (Figure S3). Therefore, we hypothesized that these cells express other αGlcNAc-binding proteins and searched for them in AGS cells by WB with an anti-αGlcNAc Ab. We detected two main bands, one near the top of the gel and the other at approximately 300 kDa in the presence of Dox (Figure S4) and used GSL II-conjugated agarose for pull-down analysis in AGS-A cell extracts. We eluted GSL II-conjugated agarose-bound proteins with *N*-acetylglucosamine and carried out SDS-PAGE followed by silver staining and WB with anti-αGlcNAc Ab. We then cut bands from silver-stained gels corresponding to bands seen in WB of Dox-treated cell extracts (Figure 4A,B), undertook in-gel trypsin digestion, and analyzed products by liquid chromatograph–mass spectrometry. The top band contained MUC1, while two bands at approximately 300 kDa contained PODXL (Table 1). To confirm that αGlcNAc binds these proteins, we undertook IP analysis in AGS-A cell lysates using anti-MUC1-N Ab and WB

TABLE 1 Peptides identified from SDS-PAGE bands shown in Figure 4A

Band of SDS-PAGE	Protein name	Accession number	Identified peptide
a	Mucin-1	P15941	DISEMFLQIYK
			QGGFLGLSNIK
b	Podocalyxin	O00592	LASVPGSQTVVVK
			ATFNPAQDK
			LGDQGPPEEAEDR
			LISLICR
			CEDLETQTQSEK
			LPAKDVYER
			EAGVSDMK
			VVSLNGELGDSWIVPLDNLTKDDLDEEEDTHL
			DDLDEEEDTHL
c	Podocalyxin	O00592	LASVPGSQTVVVK
			ATFNPAQDK
			LGDQGPPEEAEDR
			LISLICR
			CEDLETQTQSEK
			LPAKDVYER

Note: Excluded from this table are keratin and peptides from nonhuman species.

with anti-αGlcNAc Ab. That analysis revealed a band near the top of the gel in the Dox group but not present in controls (Figure 4C, left two panels). Conversely, IP with anti-αGlcNAc-conjugated latex beads and WB with anti-MUC1-N Ab revealed bands of the same molecular weight (Figure 4C, right two panels). We then carried out a compalable analysis using anti-PODXL Ab and anti-αGlcNAc Ab, and observed a band at approximately 300 kDa in Dox but not in control samples (Figure 4D). These results indicate that αGlcNAc is bound to MUC1 and PODXL in AGS-A cells.

3.6 | Colocalization of αGlcNAc with MUC1 or PODXL in AGS-A cells and human gastric cancer specimens

We then assessed subcellular localization of MUC1 and PODXL and their potential colocalization with αGlcNAc. Immunocytochemistry indicated that MUC1 localized to the plasma membrane of AGS-A cells and appeared to colocalize with αGlcNAc in the presence of Dox (Figure 4E). In clinical samples of human gastric cancer tissues, the majority of αGlcNAc is barely expressed in cancer cells.[9] However, the present study revealed that MUC1 appeared to colocalize with partially remaining αGlcNAc in the plasma membrane (Figure 4F). In contrast, PODXL localized to the cytoplasm of AGS-A cells and partially colocalized with αGlcNAc following Dox treatment (Figure 4G). In human gastric cancer specimens, PODXL also appeared to partially colocalize with partially remaining αGlcNAc in the cytoplasm (Figure 4H). These results suggest that in human gastric cancer cells, αGlcNAc binds to MUC1 at the plasma membrane and partially binds to PODXL in the cytoplasm.

3.7 | α1,4-Linked *N*-acetylglucosamine bound to MUC1 in murine normal gastric mucosa

We next examined αGlcNAc binding to MUC1 and PODXL in murine gastric mucosa. As anti-mouse MUC1-N is not available and Bäckström et al.[13] reported that immunoprecipitated products by anti-MUC1-C contains MUC1-N, we used anti-MUC1-C Ab for IP and WB analysis of αGlcNAc binding to murine MUC1. When we undertook IP in murine gastric mucosa lysates using anti-MUC1-C Ab and WB with anti-αGlcNAc Ab, and observed two bands at approximately 460 kDa and near the top of the gel in WT mice but not in *A4gnt* KO mice (Figure 5A), which completely lacked αGlcNAc.[8] The band at approximately 460 kDa was predicted to be αGlcNAc-bound MUC1-N. Conversely, pull-down with GSL II-conjugated agarose beads and WB with anti-MUC1-C Ab revealed bands of MUC1-C in WT mice but faint bands in *A4gnt* KO mice (Figure 5B).

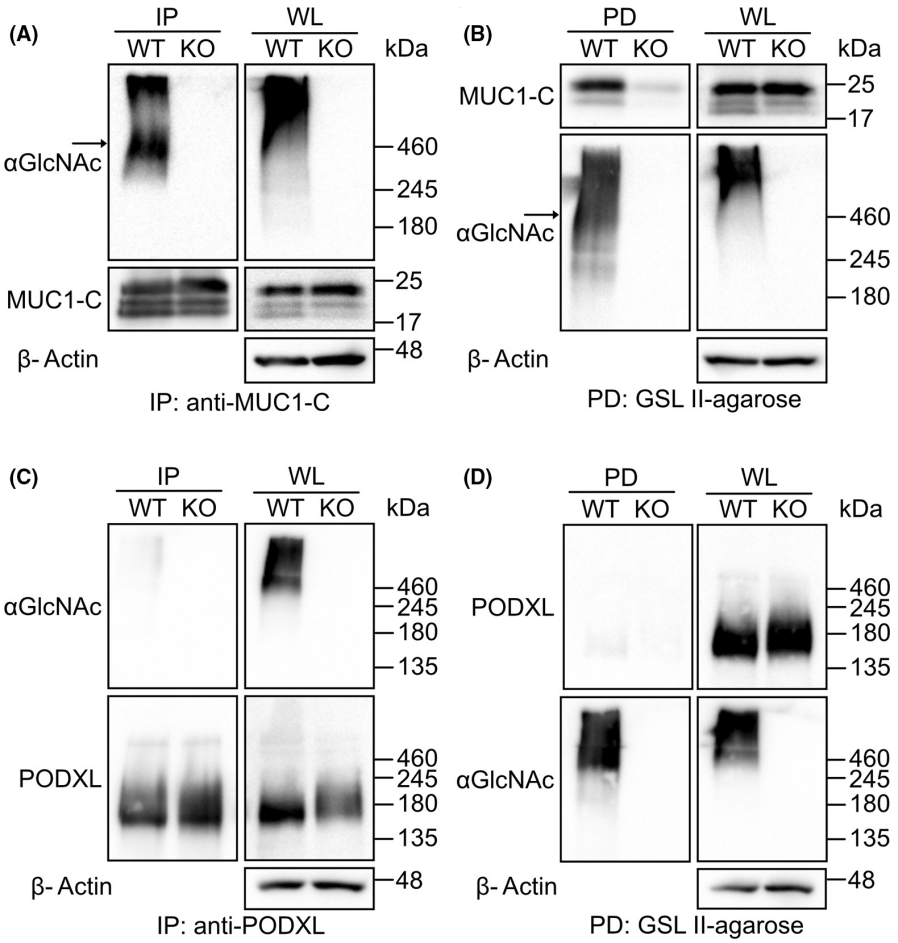

FIGURE 5 Analysis of α1,4-linked *N*-acetylglucosamine (αGlcNAc)-binding proteins in murine gastric mucosa. (A,B) Immunoprecipitation (IP) or pull-down (PD) and western blot analysis of αGlcNAc binding to Mucin-1 (MUC1). Whole lysates (WL) of indicated murine gastric mucosa were (A) immunoprecipitated with anti-MUC1-C terminus (MUC1-C) Ab or (B) pulled down with *Griffonia (Bandieraea) simplicifilia* lectin II (GSL II)-agarose and immunoblotted with indicated Abs. Arrowed bands were predicted to be αGlcNAc-bound MUC1-N terminus (MUC1-N). (C,D) IP or PD and western blot analysis of αGlcNAc binding to podocalyxin (PODXL). Whole lysates of indicated murine gastric mucosa were (C) immunoprecipitated with anti-mouse PODXL Ab or (D) pulled down with GSL II-agarose and immunoblotted with indicated Abs. αGlcNAc-bound PODXL was not detected. β-Actin served as a loading control. KO, *A4gnt* KO mice; WT, WT mice.

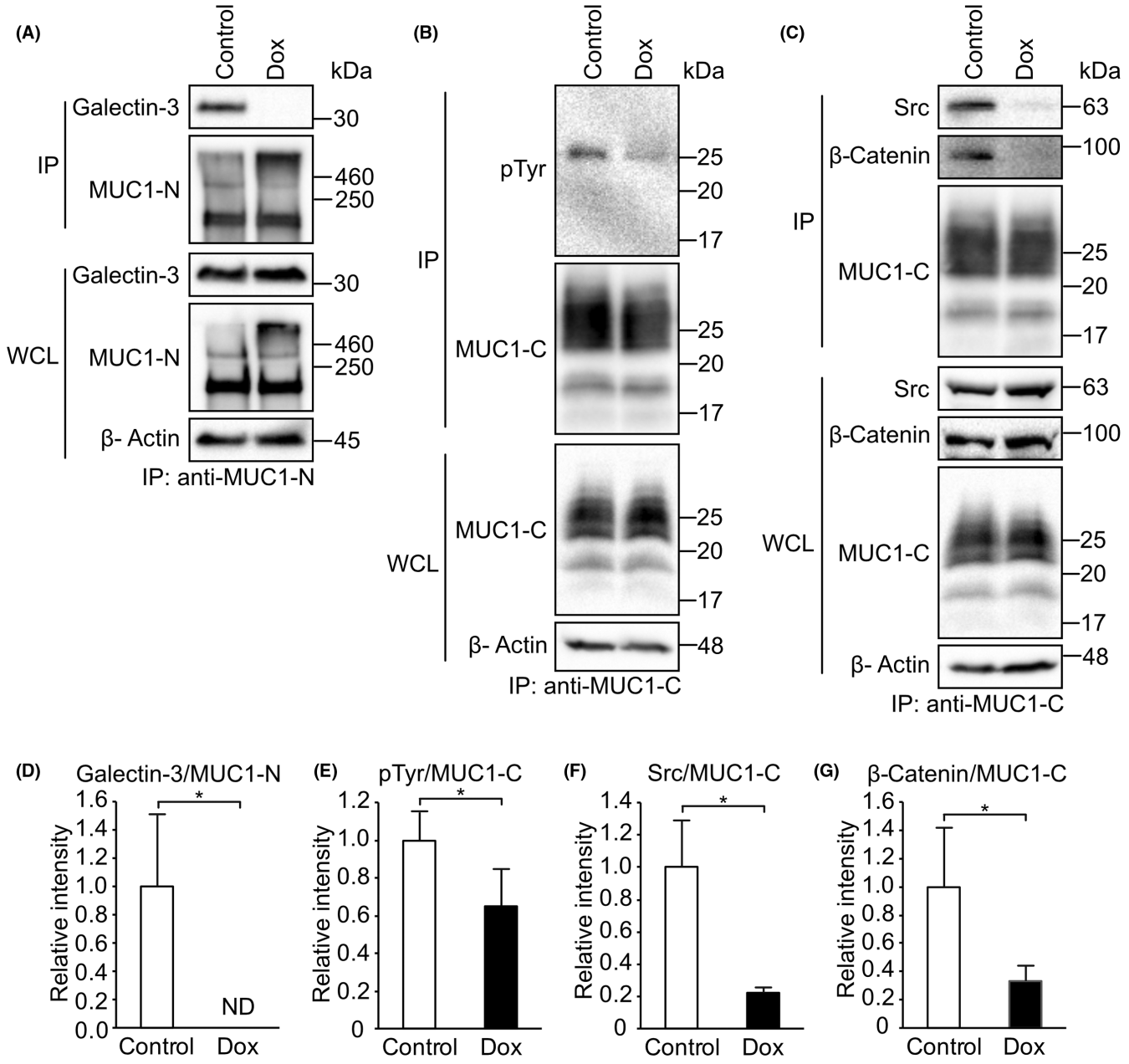

FIGURE 6 Analysis of Mucin-1 (MUC1)-binding proteins and phosphorylation. (A) Binding analysis of MUC1-N terminus (MUC1-N) and galectin-3. Whole cell lysates (WCL) of AGS-A cells were immunoprecipitated (IP) with anti-MUC1-N and immunoblotted with anti-galectin-3. (B) Phosphorylation analysis of MUC1-C terminus (MUC1-C). WCL of AGS-A cells were immunoprecipitated with anti-MUC1-C and immunoblotted with anti-phospho-tyrosine (pTyr). (C) Analysis of MUC1-C-binding proteins. WCL of AGS-A cells were immunoprecipitated with anti-MUC1-C and immunoblotted with anti-β-catenin and anti-Src Abs. β-Actin served as a loading control. (D–G) Quantification of the relative intensities of coimmunoprecipitated products to immunoprecipitated MUC1-N (D) or MUC1-C (E–G). Relative values of binding proteins or pTyr shown in the figure to the immunoprecipitated proteins were determined and the value of control cells was set to 1. Results are indicated as means, and error bars indicate SD ($n = 4$). *$p < 0.05$. ND, not detected.

This pull-down product also showed the band at approximately 460 kDa by WB with anti-αGlcNAc Ab in WT mice but not in *A4gnt* KO mice (Figure 5B). We undertook further compalable analysis using anti-PODXL Ab and anti-αGlcNAc Ab, but could not detect any αGlcNAc-bound PODXL bands at all (Figure 5C,D). These results indicate that αGlcNAc binds to MUC1 but not to PODXL in murine normal gastric mucosa.

3.8 | Effects of αGlcNAc binding on MUC1 signaling

Given these findings, we focused primarily on αGlcNAc binding to MUC1 on the plasma membrane of human gastric cancer cells and lysates of murine normal gastric mucosa. Binding of galectin-3 to MUC1-N reportedly promotes MUC1-C phosphorylation,

enabling protein interactions that activate downstream signaling.[14,15] Therefore, we analyzed galectin-3 binding to MUC1-N by IP with anti-MUC1 Ab and WB with anti-galectin-3 Ab. In standard culture conditions, we did not observe galectin-3 binding to MUC1 (data not shown) but when cells were cultured on Matrigel-coated dishes, galectin-3/MUC1 binding was detected in control cells but was significantly attenuated in the presence of Dox (Figure 6A,D). We then analyzed MUC1 signaling using extracts from AGS-A cells cultivated in Matrigel-coated dishes and observed significantly decreased MUC1-C phosphorylation in the presence of Dox (Figure 6B,E). c-Src reportedly phosphorylates MUC1-C, increasing binding of MUC1-C to β-catenin.[16,17] When we analyzed binding of Src and β-catenin to MUC1-C by IP, we observed significantly decreased Src and β-catenin binding to MUC1-C in the presence of Dox (Figure 6C,F,G). Moreover, we found that galectin-3 binding to MUC1 was significantly enhanced in the gastric mucosa of *A4gnt* KO mice compared to WT mice (Figure 7). These results suggest that the galactose terminus of MUC1-N, an important sugar residue for galectin-3 binding, could be glycosylated by αGlcNAc, thereby inhibiting galectin-3 binding to MUC1-N and attenuating downstream MUC1 signaling.

4 | DISCUSSION

In this study, we showed that enhancing αGlcNAc biosynthesis attenuates cellular proliferation, motility, and invasiveness of the moderately differentiated gastric adenocarcinoma cell line AGS and the well differentiated gastric adenocarcinoma cell line MKN7 in vitro. We also showed that AGS cell tumorigenesis is suppressed by αGlcNAc in a xenograft model. Relevant to the molecular basis of these phenotypes, we identified MUC1 and PODXL as αGlcNAc-binding proteins, and αGlcNAc binding to MUC1 decreased its downstream signaling. These findings suggest that αGlcNAc acts as a tumor suppressor by inhibiting MUC1 signaling.

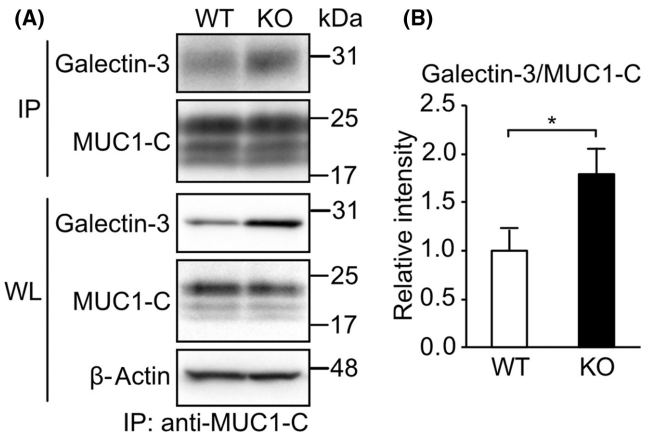

FIGURE 7 Analysis of galectin-3 binding to Mucin-1 (MUC1) in murine gastric mucosa. (A) Binding analysis of MUC1 and galectin-3. Whole lysates (WL) of murine gastric mucosa were immunoprecipitated (IP) with anti-MUC1-C terminus (MUC1-C) and immunoblotted with anti-galectin-3. β-Actin served as a loading control. KO, *A4gnt* KO mice; WT, WT mice. (B) Quantification of the relative intensities of galectin-3 to MUC1-C. The relative values of coimmunoprecipitated galectin-3 to immunoprecipitated MUC1-C were determined and the value of WT mice was set to 1. Results are indicated as means, and error bars indicate SD ($n = 3$). $^*p < 0.05$.

Previously, we reported that *A4gnt* KO mice show complete loss of αGlcNAc and spontaneously develop differentiated-type gastric adenocarcinoma.[8] We also reported that αGlcNAc loss is associated with poor prognosis of differentiated-type gastric adenocarcinoma patients.[9] To define αGlcNAc function in gastric cancer development, we upregulated its biosynthesis through ectopic expression of α4GnT using the Tet-On system in the gastric cancer cell lines AGS and MKN7. We detected that the forced expression of αGlcNAc suppressed cellular proliferation in both cell lines in vitro (see Figures 1C–E and S1C). Moreover, we showed that tumorigenesis of AGS cells is suppressed by αGlcNAc overexpression in a xenograft model (see Figure 3), in agreement with spontaneous development of differentiated-type gastric adenocarcinoma seen in *A4gnt* KO mice.[8] The above lines of evidence indicate that αGlcNAc acts as a tumor suppressor in vitro and in vivo.

We previously reported that αGlcNAc is frequently downregulated in samples from patients with differentiated-type gastric adenocarcinoma and observed that loss significantly correlated with depth of invasion, venous invasion, and stage.[9,12] Previous reports show that αGlcNAc is primarily attached to MUC6 in gastric mucosa.[4–6] Accumulating evidence indicates that αGlcNAc loss is an early event of cancer development in several gastric mucin-producing tumors including stomach tumors,[6,9–12,18–23] and MUC6 expression is subsequently suppressed at late stages of tumor development.[20,22,23] We recently showed that ectopic MUC6 expression attenuates malignant phenotypes in MIA PaCa-2 and PANC-1 pancreatic cancer cell lines, and that coexpression of α4GnT further attenuates these malignant phenotypes in vitro.[24] These findings strongly suggest that αGlcNAc binding to MUC6 has tumor suppressive effects. Here, we also observed that αGlcNAc overexpression attenuates cellular motility and invasiveness with cytoskeletal disruption of AGS cells (see Figures 2B–E,G, and S2B–E). However, MUC6 is not expressed in AGS or MKN7 cells (see Figure S3), thus we searched for other proteins in AGS cells that bind αGlcNAc and antagonize tumor malignancy. That search revealed two αGlcNAc binding proteins, MUC1 and PODXL, in AGS cells (see Figure 4A–D and Table 1). MUC1 and PODXL colocalized with αGlcNAc in AGS cells (see Figure 4E,G) and human gastric cancer cells in the patients (see Figure 4F,H). MUC1 reportedly functions in the development of various cancers,[25,26] including gastric cancer,[27–29] as does PODXL.[30,31] We also observed that the molecular weight of PODXL was decreased by Dox treatment (see Figure 4D, far left and far right panels), suggesting that αGlcNAc binding to PODXL might shorten its sugar chains. However, αGlcNAc binding to PODXL was not detected in murine normal gastric mucosa (see Figure 5C,D). These results suggest that the significance of αGlcNAc-binding to PODXL differs by species.

In this study, we established α4GnT expressing cells using the Tet-On system. In the process of preparing both AGS and MKN7 cell

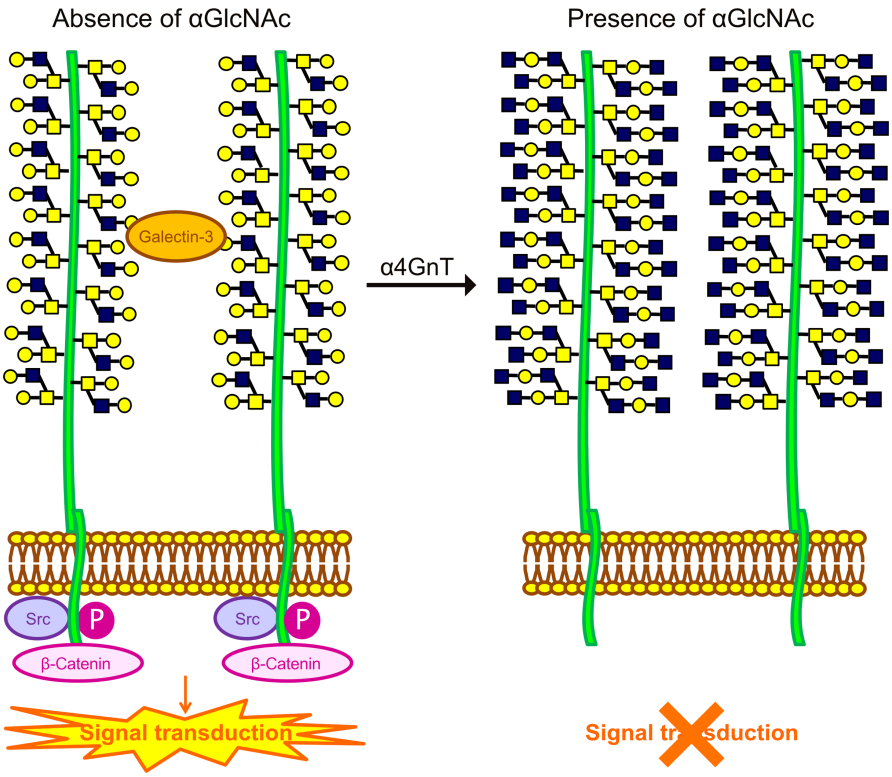

FIGURE 8 Schematic showing inhibitory effects of α1,4-linked *N*-acetylglucosamine (αGlcNAc) binding to Mucin-1 (MUC1). In the absence of αGlcNAc, galactose on MUC1 is exposed and galectin-3 binds to galactose residues on MUC1-N terminus (MUC1-N), activating downstream signaling. When αGlcNAc biosynthesis is upregulated by α4GnT activity, *N*-acetylglucosamine binds to galactose on MUC1 with a α1,4-linkage, and galectin-3 cannot bind MUC1-N. Therefore, signal transduction is blocked.

pools, we selected populations in which αGlcNAc is highly expressed at the cell surface. We found that αGlcNAc colocalizes with MUC1 on the plasma membrane of AGS cells and human gastric cancer cells (see Figure 4E,F). We also found that αGlcNAc is bound to MUC1 present in murine normal gastric mucosa (see Figure 5A,B). Thus, we focused on MUC1. We found that αGlcNAc binding to MUC1 significantly decreased both galectin-3 binding to MUC1-N (see Figure 6A,D) and phosphorylation of MUC1-C (see Figure 6B,E). Moreover, Src and β-catenin binding to MUC1-C was significantly attenuated by αGlcNAc binding to MUC1 (see Figure 6C,E,F). We further showed that galectin-3 binding to MUC1 was significantly enhanced in the gastric mucosa of *A4gnt* KO mice, which completely lacked αGlcNAc and developed differentiated-type adenocarcinoma, compared to WT mice (see Figure 7A,B). As AGS cells express β-1,6-*N*-acetylglucosaminyltransferase (C2GnT) (Figure S5), which catalyzes initiation of synthesis of the core 2 structure, αGlcNAc is on core 2 structure in this cell line. Furthermore, we propose that when αGlcNAc is absent on the *O*-glycan of MUC1-N, galectin-3 binds to MUC1-N to activate downstream signal transduction. However, when αGlcNAc is present, *N*-acetylglucosamine binds to galactose with α1,4-linkage, and galectin-3 cannot bind MUC1-N, blocking signal transduction and inhibiting cell proliferation, motility, invasiveness, and tumorigenesis (Figure 8). Al Masri et al.[32] reported that formation of a MUC1-C/Src complex activates Src signaling and enhances cell invasion and proliferation in a mouse mammary tumor model. Moreover, Schroeder et al. reported that a complex of MUC1-C and β-catenin enhances cellular invasiveness by interacting with Vinculin and Fascin in breast cancer.[33,34] These reports are consistent with our results.

In conclusion, glycosylation of MUC1 by αGlcNAc attenuates its downstream signaling, decreasing cell proliferation, motility, invasiveness, and tumorigenesis. These results suggest that αGlcNAc regulates cancer cell malignancy and could serve as a useful diagnostic biomarker of malignancy.

ACKNOWLEDGMENTS

We thank Mr. Hiroyuki Matsuura for collection of gastric cancer specimens and Dr. Elise Lamar for editing the manuscript. This work was supported by Grants-in-Aid for Scientific Research (KAKENHI) from the Japan Society for the Promotion of Science to C. Fujii (18K08613) and J. Nakayama (19H03441).

FUNDING INFORMATION

Japan Society for the Promotion of Science (KAKENHI), Grant/Award Number: 18K08613, 19H03441.

DISCLOSURE

The authors have no conflict of interest.

ETHICS STATEMENT

Approval of the research protocol by an institutional review board: Analysis of human gastric cancer specimens was approved by the Ethics Committee of the Shinshu University School of Medicine, Matsumoto, Japan, and Iiyama Red Cross Hospital, Iiyama, Japan, and carried out in accordance with the Helsinki Declaration of 1964 and later versions.

Informed consent: Informed consent was obtained in the form of an opt-out on the website.

Registry and registration no. of the study: Shinshu University School of Medicine no. 4874 and Iiyama Red Cross Hospital no. 2020-10.

Animal studies: All animal experiments were carried out with approval of the Institutional Animal Care and Use Committee of Shinshu University School of Medicine, Matsumoto, Japan (nos. 300049-1 and 021058).

ORCID

Chifumi Fujii https://orcid.org/0000-0001-8735-5274
Masatomo Kawakubo https://orcid.org/0000-0001-5106-5742
Jun Nakayama https://orcid.org/0000-0001-6773-2802

REFERENCES

1. Bray F, Laversanne M, Weiderpass E, Soerjomataram I. The ever-increasing importance of cancer as a leading cause of premature death worldwide. *Cancer*. 2021;127:3029-3030.
2. Sung H, Ferlay J, Siegel RL, et al. Global cancer statistics 2020: GLOBOCAN estimates of incidence and mortality worldwide for 36 cancers in 185 countries. *CA Cancer J Clin*. 2021;71:209-249.
3. Joshi SS, Badgwell BD. Current treatment and recent progress in gastric cancer. *CA Cancer J Clin*. 2021;71:264-279.
4. Ishihara K, Kurihara M, Goso Y, et al. Peripheral α-linked *N*-acetylglucosamine on the carbohydrate moiety of mucin derived from mammalian gastric gland mucous cells: epitope recognized by a newly characterized monoclonal antibody. *Biochem J*. 1996;318:409-416.
5. Zhang MX, Nakayama J, Hidaka E, et al. Immunohistochemical demonstration of α 1,4-*N*-acetylglucosaminyltransferase that forms GlcNAcα1,4Galβ residues in human gastrointestinal mucosa. *J Histochem Cytochem*. 2001;49:587-596.
6. Nakayama J. Dual roles of gastric gland mucin-specific *O*-glycans in prevention of gastric cancer. *Acta Histochem Cytochem*. 2014;47:1-9.
7. Nakayama J, Yeh JC, Misra AK, Ito S, Katsuyama T, Fukuda M. Expressioncloningofahumanα1,4-*N*-acetylglucosaminyltransferase that forms GlcNAcα1→4Galβ→R, a glycan specifically expressed in the gastric gland mucous cell-type mucin. *Proc Natl Acad Sci U S A*. 1999;96:8991-8996.
8. Karasawa F, Shiota A, Goso Y, et al. Essential role of gastric gland mucin in preventing gastric cancer in mice. *J Clin Invest*. 2012;122:923-934.
9. Shiratsu K, Higuchi K, Nakayama J. Loss of gastric gland mucin-specific *O*-glycan is associated with progression of differentiated-type adenocarcinoma of the stomach. *Cancer Sci*. 2014;105:126-133.
10. Yamada S, Okamura T, Kobayashi S, Tanaka E, Nakayama J. Reduced gland mucin-specific *O*-glycan in gastric atrophy: A possible risk factor for differentiated-type adenocarcinoma of the stomach. *J Gastroenterol Hepatol*. 2015;30:1478-1484.
11. Yamanoi K, Sekine S, Higuchi K, Kushima R, Nakayama J. Decreased expression of gastric gland mucin-specific glycan α1,4-linked *N*-acetylglucosamine on its scaffold mucin 6 is associated with malignant potential of pyloric gland adenoma of the stomach. *Histopathology*. 2015;67:898-904.
12. Yamanoi K, Nakayama J. Reduced αGlcNAc glycosylation on gastric gland mucin is a biomarker of malignant potential for gastric cancer, Barrett's adenocarcinoma, and pancreatic cancer. *Histochem Cell Biol*. 2018;149:569-575.
13. Bäckström M, Thomsson K, Karlsson H, Hansson G. Sensitive liquid chromatography-electrospray mass spectrometry allows for the analysis of the *O*-glycosylation of immunoprecipitated proteins from cells or tissues: application to MUC1 glycosylation in cancer. *J Proteome Res*. 2009;8:538-545.
14. Tanida S, Mori Y, Ishida A, Akita K, Nakada H. Galectin-3 binds to MUC1-N-terminal domain and triggers recruitment of β-catenin in MUC1-expressing mouse 3T3 cells. *Biochim Biophys Acta*. 2014;1840:1790-1797.
15. Mori Y, Akita K, Yashiro M, et al. Binding of galectin-3, a β-galactoside-binding lectin, to MUC1 protein enhances phosphorylation of extracellular signal-regulated kinase 1/2 (ERK1/2) and Akt, promoting tumor cell malignancy. *J Biol Chem*. 2015;290:26125-26140.
16. Li Y, Kuwahara H, Ren J, Wen G, Kufe D. The c-Src tyrosine kinase regulates signaling of the human DF3/MUC1 carcinoma-associated antigen with GSK3β and β-catenin. *J Biol Chem*. 2001;276:6061-6064.
17. Senapati S, Das S, Batra SK. Mucin-interacting proteins: from function to therapeutics. *Trends Biochem Sci*. 2010;35:236-245.
18. Iwaya Y, Hasebe O, Koide N, et al. Reduced expression of αGlcNAc in Barrett's oesophagus adjacent to Barrett's adenocarcinoma – a possible biomarker to predict the malignant potential of Barrett's oesophagus. *Histopathology*. 2014;64:536-546.
19. Ohya A, Yamanoi K, Shimojo H, Fujii C, Nakayama J. Gastric gland mucin-specific *O*-glycan expression decreases with tumor progression from precursor lesions to pancreatic cancer. *Cancer Sci*. 2017;108:1897-1902.
20. Yamanoi K, Ishii K, Tsukamoto M, Asaka S, Nakayama J. Gastric gland mucin-specific *O*-glycan expression decreases as tumor cells progress from lobular endocervical gland hyperplasia to cervical mucinous carcinoma, gastric type. *Virchows Arch*. 2018;473:305-311.
21. Ida K, Yamanoi K, Asaka S, et al. αGlcNAc and its catalyst α4GnT are diagnostic and prognostic markers in uterine cervical tumor, gastric type. *Sci Rep*. 2019;9:13043.
22. Okumura M, Yamanoi K, Uehara T, Nakayama J. Decreased α-1,4-linked *N*-acetylglucosamine glycosylation in biliary tract cancer progression from biliary intraepithelial neoplasia to invasive adenocarcinoma. *Cancer Sci*. 2020;111:4629-4635.
23. Ohya A, Matoba H, Fujinaga Y, Nakayama J. Decreased gastric gland mucin-specific *O*-glycans are involved in the progression of ovarian primary mucinous tumours. *Acta Histochem Cytochem*. 2021;54:115-122.
24. Yuki A, Fujii C, Yamanoi K, et al. Glycosylation of MUC6 by α1,4-linked *N*-acetylglucosamine enhances suppression of pancreatic cancer malignancy. *Cancer Sci*. 2022;113:576-586.
25. Nath S, Mukherjee P. MUC1: a multifaceted oncoprotein with a key role in cancer progression. *Trends Mol Med*. 2014;20:332-342.
26. Hanson RL, Hollingsworth MA. Functional consequences of differential *O*-glycosylation of MUC1, MUC4, and MUC16 (Downstream effects on signaling). *Biomolecules*. 2016;6:34.
27. Jia Y, Persson C, Hou L, et al. A comprehensive analysis of common genetic variation in MUC1, MUC5AC, MUC6 genes and risk of stomach cancer. *Cancer Causes Control*. 2010;21:313-321.
28. Tamura Y, Higashi M, Kitamoto S, et al. MUC4 and MUC1 expression in adenocarcinoma of the stomach correlates with vessel invasion and lymph node metastasis: an immunohistochemical study of early gastric cancer. *PLoS One*. 2012;7:e49251.
29. Saeki N, Sakamoto H, Yoshida T. Mucin 1 gene (MUC1) and gastric-cancer susceptibility. *Int J Mol Sci*. 2014;15:7958-7973.
30. Zhi Q, Chen H, Liu F, et al. Podocalyxin-like protein promotes gastric cancer progression through interacting with RUN and FYVE domain containing 1 protein. *Cancer Sci*. 2019;110:118-134.
31. Zhang J, Zhu Z, Wu H, et al. PODXL, negatively regulated by KLF4, promotes the EMT and metastasis and serves as a novel prognostic indicator of gastric cancer. *Gastric Cancer*. 2019;22:48-59.
32. Al Masri A, Gendler SJ. Muc1 affects c-Src signaling in PyV MT-induced mammary tumorigenesis. *Oncogene*. 2005;24:5799-5808.

33. Schroeder JA, Adriance MC, Thompson MC, Camenisch TD, Gendler SJ. MUC1 alters β-catenin-dependent tumor formation and promotes cellular invasion. *Oncogene*. 2003;22:1324-1332.
34. Pai P, Rachagani S, Dhawan P, Batra SK. Mucins and Wnt/β-catenin signaling in gastrointestinal cancers: an unholy nexus. *Carcinogenesis*. 2016;37:223-232.

SUPPORTING INFORMATION

Additional supporting information can be found online in the Supporting Information section at the end of this article.

How to cite this article: Fujii C, Harumiya S, Sato Y, Kawakubo M, Matoba H, Nakayama J. α1,4-Linked *N*-acetylglucosamine suppresses gastric cancer development by inhibiting Mucin-1-mediated signaling. *Cancer Sci*. 2022;113:3852-3863. doi: 10.1111/cas.15530